

DATA ASSIMILATION TSUNAMI FORECASTING USING RADIAL FLOW VELOCITY DISTRIBUTION WITH A SINGLE OCEAN RADAR

KANETO TOSHIMICHI

Tokyo Electric Power Company Holdings, Inc., Tokyo, Japan, kaneto.toshimichi@tepcoco.jp

KIMURA TATSUTO

Tokyo Electric Power Services Co., Ltd., Tokyo, Japan, kimura_tatsu@tepscoco.jp

TERAOKA SHUNSUKE

Tokyo Electric Power Company Holdings, Inc., Tokyo, Japan, teraoka.shunsuke@tepcoco.jp

ABSTRACT

We examined real-time tsunami forecasting based on the data assimilation method using the radial flow velocity distribution observed with a single ocean radar installed at the Kashiwazaki-Kariwa Nuclear Power Station. In order to simulate the radial flow velocity observation at the time of tsunami occurrence, we used a virtual tsunami observation value in which the radial flow velocity from a tsunami numerical simulation is synthesized with the observed velocity from an ocean radar. In the data assimilation tsunami forecasting, the nonlinear long wave theory was used for the tsunami numerical simulation, and the optimal interpolation method was used for the data assimilation. By comparing the tsunami waveforms at the site obtained by the tsunami numerical simulation from the assumed tsunami source, and that obtained by tsunami forecasting using the virtual tsunami observation value, the practical applicability of data assimilation tsunami forecasting with a single ocean radar was confirmed.

Keywords: tsunami forecasting, data assimilation, ocean radar, HF radar, long wave theory

1. INTRODUCTION

Ocean radars irradiate HF band radio-waves from an inland base station and receive backscattered waves. There are expectations for the use of ocean radars in tsunami detection systems, because they can measure the radial flow velocity by analyzing the radio-waves received (Barrick, 1979). In fact, ocean radar observed the 2011 off the Pacific coast of the Tohoku Earthquake tsunami (Hinata et al., 2011; Lipa et al., 2011) and the 2012 Sumatra Island off the coast of Earthquake tsunami (Lipa et al., 2012), demonstrating the possibility of tsunami detection.

We examined real-time tsunami forecasting based on the data assimilation method using the radial flow velocity distribution observed with a single ocean radar installed at the Kashiwazaki-Kariwa Nuclear Power Station.

Kimura et al. (2018) reported a tsunami forecasting method using only the radial flow velocity distribution observed with a single ocean radar. However, in Kimura et al. (2018), the radial flow velocity distribution is obtained via a tsunami numerical simulation, and it has not been verified using actual tsunami observation values.

Therefore, we considered verifying the tsunami forecasting using actual observation values in practice. In this study, first of all, to assume the radial flow velocity distribution in a real tsunami, we combined the radial flow velocity distribution obtained by the tsunami numerical simulation with the usual radial flow velocity distribution observed by a single ocean radar installed at the Kashiwazaki-Kariwa Nuclear Power Station (hereinafter, this is called a "virtual tsunami observation value").

Next, we performed tsunami forecasting based on data assimilation using this virtual tsunami observation value and examined the applicability of this tsunami forecasting method in practice.

2. TSUNAMI FORECASTING USING DATA ASSIMILATION METHOD

In this study, in terms of computational load, we used the optimal interpolation method (Awaji et al., 2009), with the error information of the background field not varying with time, as the data assimilation method, as per

Kimura et al. (2018). In the optimal interpolation method, the optimal estimated value \mathbf{x}^a is given by the weighted average of the predicted value (simulation result) \mathbf{x}^b and the observed value \mathbf{y} , as shown in the following formula.

$$\mathbf{x}^a = \mathbf{x}^b + \mathbf{W}[\mathbf{y} - \mathbf{H}\mathbf{x}^b] \quad (1)$$

Here, \mathbf{W} is the weight matrix, and \mathbf{H} is the observation matrix. The observation matrix \mathbf{H} is a transformation matrix from the physical quantity \mathbf{x} at the computational grid point to the physical quantity \mathbf{y} observed at the observation point. The calculation method of the weight matrix \mathbf{W} followed Kimura et al. (2018). However, to consider noise in the actual observations, the ratio of the observation error standard deviation to the background error standard deviation was set to 4.

The flow of the tsunami numerical simulation using data assimilation is as follows.

- (1) calculate the weight matrix \mathbf{W}
- (2) perform a tsunami numerical simulation based on the estimated value \mathbf{x}^a_{n-1} to obtain the forecast value \mathbf{x}^b_n
- (3) based on the difference between the forecast value \mathbf{x}^b_n and the observed value \mathbf{y}_n , correct the forecast value \mathbf{x}^b_n and obtain the estimated value \mathbf{x}^a_n (Equation (1)).

The estimated value \mathbf{x}^a is updated by repeating (2) and (3).

The component of \mathbf{x} is the water level η and the flow rate per unit width M and N at each grid point, and the component of \mathbf{y} is the radial flow velocity u_r observed by an ocean radar at each observation point. The initial values of the water level and the flow rate per unit width M and N were set to 0. The components of the observation matrix \mathbf{H} include the conversion from the linear flow rate to the flow velocity. However, since \mathbf{H} is a linear matrix, it was converted using the still water depth h instead of the total water depth ($D = h + \eta$).

3. OCEAN RADAR INSTALLED AT KASHIWAZAKI-KARIWA NUCLEAR POWER STATION

We have installed an ocean radar at Kashiwazaki-Kariwa Nuclear Power Station and conducted research on the early detection and forecasting of tsunami. The ocean radar is designed to have seismic resistance as per important nuclear power plant facilities and to be able to connect to the emergency power supply when the external power supply is lost. An ocean radar antenna was installed on the roof of the Unit 5 reactor building (altitude about 51 m), and observations have been performed since December 2018. The specifications of the ocean radar are shown in Table 1, and the installation location is shown in Figure 1.

Table 1. Ocean radar specifications.

item		specification
performance	radar system	FMICW
	observation range	30km or more
	azimuth range	120 degrees or less
	distance resolution	1.5km or less
	angular resolution	18 degrees or less
	frequency	24.515MHz
	speed resolution	10cm/s or less
	data update interval	64 sec

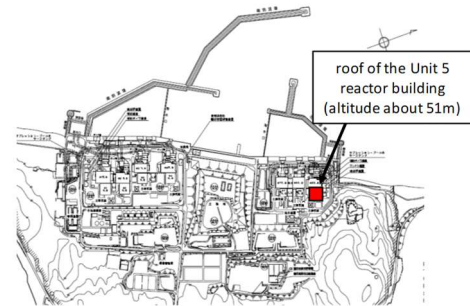


Figure 1. Ocean radar installation location.

4. RADIAL FLOW VELOCITY WITH OCEAN RADAR

It is known that the rate of data acquisition with ocean radar decreases due to waves. Therefore, we confirmed whether sufficient data could be obtained for data assimilation tsunami forecasting even during high waves. The results of the observed range during high waves on January 26 are shown (Figure 2). January 26 recorded almost maximum values of wind speed during January 2019 (average wind speed (5.8m), maximum wind speed (9.5m), and maximum instantaneous wind speed (19.8m) at Kashiwazaki). For comparison, the observed range on January 12, which recorded almost the lowest values during January (1.6 m, 3.4 m, and 4.7 m, respectively), is also shown (Figure 3). The observed range on January 26 is about two-thirds of that on January 12, and it is considered that the acquisition rate of observations decreased due to waves.

Kimura et al. (2018) set the radial flow velocity observations for data assimilation to be 2 km intervals between 10 km to 30 km from the site, with the beam angle set to 20 degree intervals between 120 degrees, and reported that if radial flow velocity is given in this range, tsunami forecasting is possible with sufficient accuracy (the total number of observation point for data assimilation is 60 points). The observation range of radial flow velocity obtained on January 26, which is considered to be a low acquisition rate for observations, is approximately 30 km from the site, at 1.5 km intervals, and the beam angle is 15 degree intervals between 120 degrees (the total number of observation point for data assimilation is 160 points). This represents sufficient observations for data assimilation. However, it is necessary to continue the observations in the future, and to confirm the data acquisition rate and observation situation when the marine conditions are more severe.

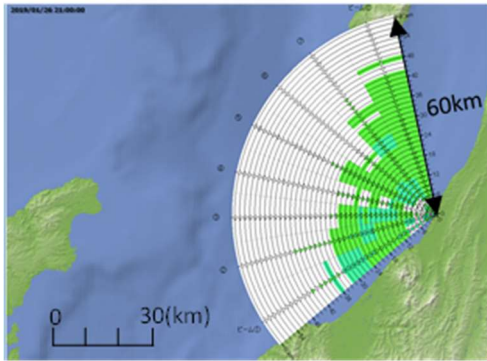


Figure 2. Ocean radar observation range. (2019/1/26 21:00)

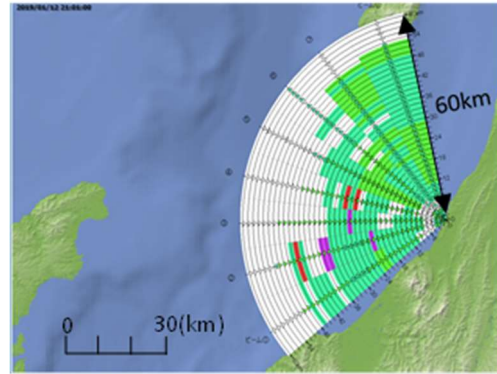


Figure 3. Ocean radar observation range. (2019/1/12 21:00)

5. VIRTUAL TSUNAMI OBSERVATION VALUE

Since we had confirmed that the observation values required for data assimilation could be obtained, in order to simulate the radial flow velocity when an actual tsunami has occurred, we combined the radial flow velocity observed via the ocean radar and the radial flow velocity obtained via the tsunami numerical simulation.

However, since the observed value contains a steady flow component (for example, wind-drive current) that cannot be calculated via a nonlinear long wave equation, this must be removed in advance.

Therefore, we removed this flow velocity component using the following two methods.

- (1) Filter out components other than the dominant frequency due to tsunami
- (2) Remove the average flow velocity for a certain period before the observation from the radial flow velocity

We consider three major tsunami sources at the Kashiwazaki-Kariwa Nuclear Power Station: a submarine active fault, a model in which two regions in the eastern margin of the Sea of Japan are broken simultaneously (hereinafter, this is called the "2-region model"), and a model in which one region in the eastern margin of the Sea of Japan is broken (hereinafter, this is called the "1-region model"). Figure 4 shows the location of the tsunami source, Table 2 shows the specifications of the tsunami source, and Figure 5 shows the calculation area for the tsunami numerical simulation using these sources.

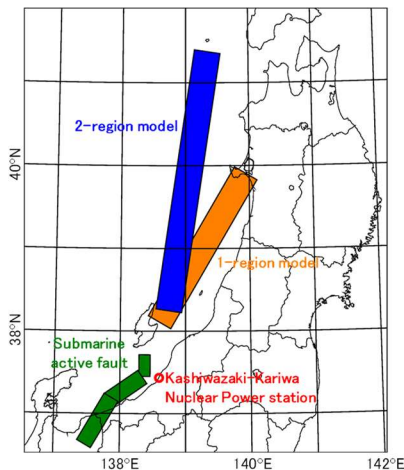


Figure 4. Tsunami sources.

Table 2. Tsunami source specifications.

Tsunami source	Mw	length (km)	width (km)	strike (°)	depth of upper edge (km)	dip angle (°)	slip angle (°)	slip amount (m)
Submarine Active fault	8.0	29.0	21.2	0.0	2.5	45.0	62.0	7.7
		55.0	26.2	55.0	2.5	35.0	96.0	7.7
		72.0	26.2	30.0	2.5	35.0	90.0	7.7
2-region model	8.6	350.0	40.0	188.0	5.0	30.0	100.0	22.3
1-region model	8.4	230.0	40.0	30.0	0.0	30.0	90.0	14.6

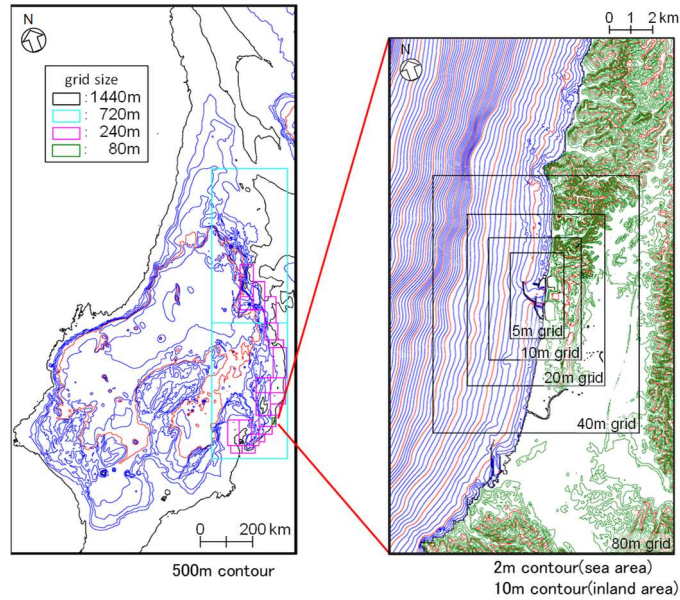


Figure 5. Computational region.

Since the predominant period of the tsunami caused by these sources is about 30 to 80 minutes, in method (1), the frequency bands of 150 seconds or less and 80 minutes or more are cut. In method (2), the average flow velocity of about 70 minutes before the observed value was obtained is removed from the observed value. The radial flow velocity obtained via the tsunami numerical simulation was rounded to the nearest 0.1m/s on account of the velocity resolution of the ocean radar.

Figure 6 to 9 show the results of applying methods (1) and (2) to observation data from January 26, 2019, with radial flow velocity from the submarine active fault, 2-region model, and 1-region model. The radial flow velocity is positive when approaching the site. There is no significant difference in the flow velocity values in any method.

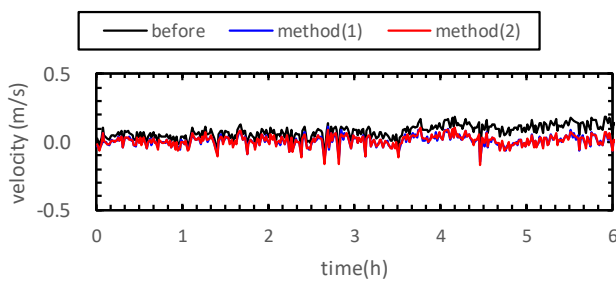


Figure 6. Observed flow velocity.
(2019/1/26, beam 4, 18 km distance)

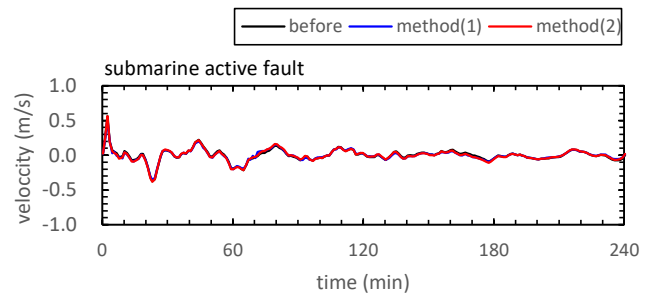


Figure 7. Tsunami velocity from the submarine active fault.
(beam 4, 18 km distance)

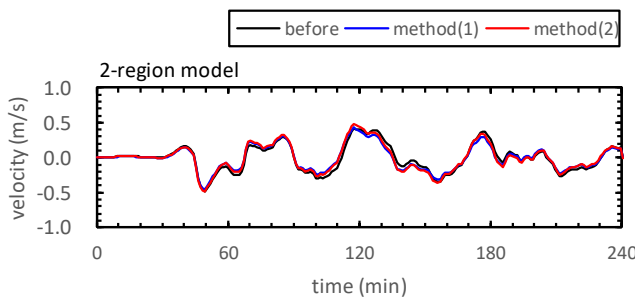


Figure 8. Tsunami velocity from 2-region model.
(beam 4, 18 km distance)

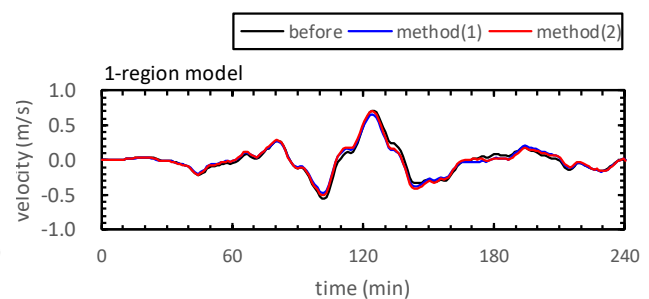


Figure 9. Tsunami velocity from 1-region model.
(beam 4, 18 km distance)

6. TSUNAMI FORECASTING BASED ON DATA ASSIMILATION METHOD USING VIRTUAL TSUNAMI OBSERVATION VALUE

We examined tsunami forecasting based on data assimilation using virtual tsunami observation values. The foundation equation of the tsunami numerical simulation is a nonlinear long wave theory, taking into account

the exposure of the seabed and run-up to land. Figure 10 shows the calculation area for data assimilation tsunami forecasting. It was limited to the vicinity of the ocean radar observation range (43.2 km east-west, 57.6 km north-south). The grid was subdivided into 240 m, 80 m, 40 m, 20 m, 10 m, and 5 m. Grid areas of 10 m or more were set to the full reflection condition, and the 5 m grid area was set to the wave front condition.

Observation points in the calculation are the same as the actual radar observation point and are placed at an interval of 1.5 km in the radial direction and 15 degrees in the circumferential direction within 120 degrees from the site. However, only points within 35 km from the site were used, and data was not assimilated at that point if observations were missing. The data assimilation interval was set at about 1 minute, which is the same as the velocity measurement interval of the ocean radar.

Figure 11 shows the output position of the results. Figure 12 to 14 show the results of the data assimilation. The correlation coefficient with the tsunami numerical simulation result is also shown. It is considered that tsunami forecasting with high accuracy is possible for any tsunami source. Tsunami caused by submarine active faults can be forecasted with very high accuracy, including subsequent waves. The accuracy of the 2-region model and 1-region model is slightly lower than the results for the submarine active fault, and the peak tsunami water level may not match, but the phases match well and, overall, it can be said that the trend of the tsunami has been forecasted.

With regard to the filter for the observed values, method (2) resulted in a slightly higher forecasting accuracy for all tsunami sources. In method (1), the peaks of the tsunami water level are forecasted to be slightly smaller, which may be due to the effects of the short-period filter.

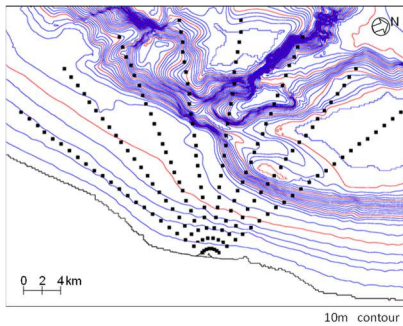


Figure 10. Data assimilation computational region.

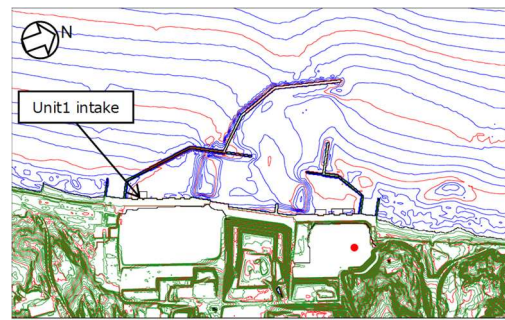


Figure 11. Output position.

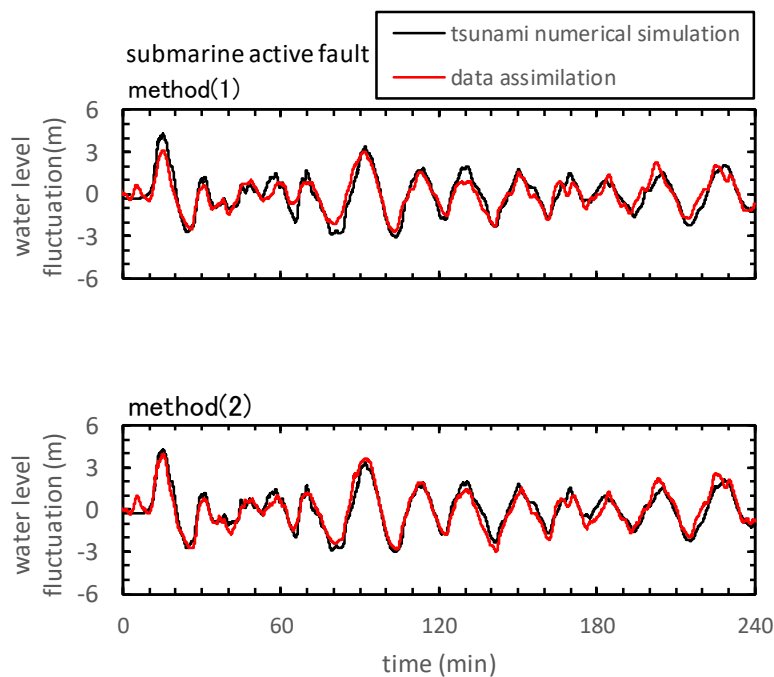


Figure 12. Data assimilation results using virtual tsunami observation value (submarine active fault).
Correlation coefficient: (1) 0.91, (2) 0.94

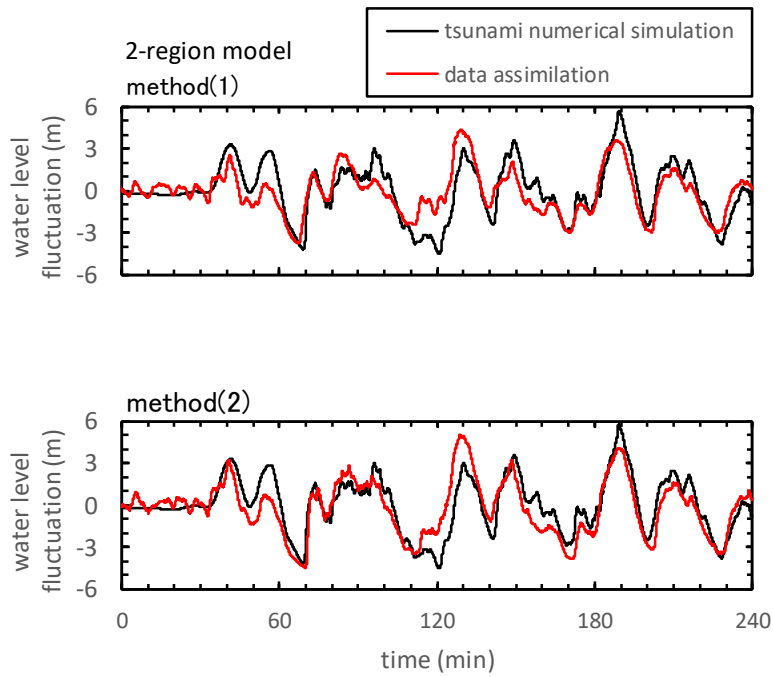


Figure 13. Data assimilation results using virtual tsunami observation value (2-region model).
Correlation coefficient: (1) 0.77, (2) 0.83

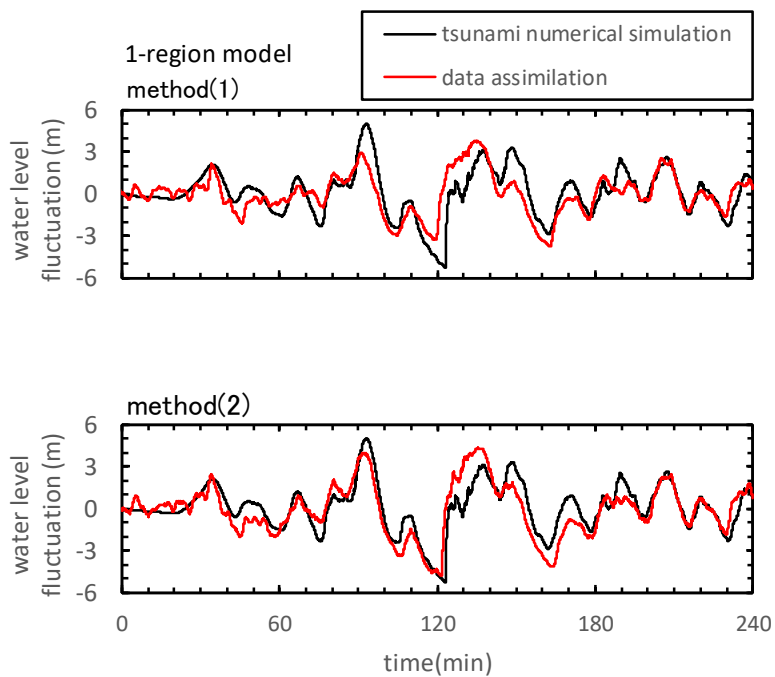


Figure 14. Data assimilation results using virtual tsunami observation value (1-region model).
Correlation coefficient: (1) 0.71, (2) 0.83

7. CONCLUSIONS

We examined the practical applicability of tsunami forecasting using a single ocean radar installed at the Kashiwazaki-Kariwa Nuclear Power Station. In order to simulate the radial flow velocity that would actually be observed when a tsunami occurs, we synthesized radial flow velocities obtained via tsunami numerical simulation with observation values of radial flow velocities at normal times, and performed tsunami forecasting based on data assimilation using a virtual tsunami observation value. As a result, it was shown that tsunami forecasting can be performed with high accuracy by setting an appropriate filter for the observed values.

REFERENCES

- Awaji, T., Kamachi, T., Ikeda, M. and Ishikawa, Y. (2009). Data assimilation, Kyoto university press, 28p. in Japanese.
- Barrick, D. E. (1979). A coastal radar system for tsunami warning, *Remote Sensing of Environment*, Vol. 8 No. 4, pp. 353-358.
- Hinata, H., Fujii, S., Furukawa, K., Kataoka, T., Miyata, M., Kobayashi, T., Mizutani, M., Kokai, T. and Kanatsu, N. (2011). Propagating tsunami wave and subsequent resonant response signals detected by HF radar in the Kii Channel, Japan, *Estuarine, Coastal and Shelf Science*, Vol. 95, No. 1, pp. 268-273.
- Kimura, T., Yamashita, K., Kaneto, T. and Masuko, M. (2018). Data assimilation tsunami forecasting using radial flow velocity distribution with ocean radar, *Journal of JSCE B2 (coastal engineering)*, Vol. 74, No. 2, pp. I_517-I_522.
- Lipa, B., Barrick, D., Saitoh, S., Ishikawa, Y., Awaji, T., Largier, J. and Garfield, N. (2011). Japan tsunami current flows observed by HF radars on two continents, *Remote Sensing*, Vol. 3, No. 3, pp. 1663-1679.
- Lipa, B., Barrick, D., Diposaptono, S., Isaacson, J., Jena, B. K., Nyden, B., Rajesh, K. and Kumar, T. S. (2012). High frequency (HF) radar detection of the weak 2012 Indonesian tsunamis, *Remote Sensing*, Vol. 4, No. 10, pp. 2944-2956.